Journal of Materials and Environmental Sciences
ISSN : 2028-2508

JMES, 2017 Volume 8, Issue 11, Page 3809-3816

http://www.jmaterenvironsci.com/

Electrochemical investigation on the corrosion of API 5L X52 carbon steel in simulated soil solutions

M. E. Ikpi[1*], B. O. Okonkwo[1]

1. Corrosion and Electrochemistry Research Laboratory, Department of Pure and Applied Chemistry, University of Calabar, Nigeria

Received 07 Nov 2016,
Revised 04 Apr 2017,
Accepted 10 Apr 2017

Keywords

- ✓ Corrosion;
- ✓ Simulating soil solution;
- ✓ electrochemical investigations;
- ✓ API 5L X52 steel

M E Ikpi
me_ikpi@yahoo.com
+234 8062893734

Abstract

Potentiodynamic polarization and electrochemical impedance spectroscopy (EIS) methods were used to investigate the corrosion behaviour of API 5L X52 carbon steel in simulated solutions of soil. The corrosion rates were estimated at different pH values (4.9, 7.0 and 9.0) and over a temperature range 30 to 50 ^{o}C. Results obtained from potentiodynamic polarization measurements revealed that the corrosion current density increases with increase in temperature signifying an increasing corrosion rate with temperature. The Polarization resistance was observed to increase with increase in the pH of the simulated solutions of soil indicative of a reduction in the corrosion rate with increasing alkaline environment. The activation energy for corrosion was found to range from 43-47 kJmol^{-1} falling within limits of the activation energy of steel corrosion in acidic soils. Nyquist plots showed capacitive loops with varying arc sizes depending on the duration of immersion and on the corrosive test solution. Impedance curves were matched against an appropriate model to obtain the parameters that characterize the corrosion process. Polarization resistance, corrosion current density and corrosion rate parameters of the carbon steel were used to evaluate the soil corrosivity.

1. Introduction

Pipelines form an integral part of the infrastructure of oil and gas production. The transportation of crude oil, natural gas and refined petroleum products are made possible through pipelines and are the preferred choice of transport were large volumes and long distances are involved. In Nigeria, pipelines are used either to transport gas and crude oil from production areas to distribution terminals or petroleum products from oil refineries and import-receiving jetties to storage depots. The over 3000 km network of pipeline in Nigeria traverses all of the nation's geo-political zones straddling the swamp belt, rain forest and the savannah grass lands, and are exposed to different climates and soil environments [1]. The failure of gas or crude oil pipeline in service results in a high degree of environmental, human and economic consequences. A recent study conducted in the Niger Delta Region of Nigeria; a coastal area of proven oil reserves of 22.5 billion barrels [2] reveals that pipelines are the major source of environmental degradation in Nigeria [3]. Communities argue that pipeline failures and subsequent leakages are the reasons for the oil spills in the area as opposed to oil companies attributing it to sabotage [4]. There is often the absence of periodic monitoring after the construction phase of any pipeline project. Monitoring is of immense importance, needed to ascertain pipeline integrity and guarantee safety of lives and the environment.

Pipelines exposed to underground conditions suffer from corrosion and cracking. External corrosion and cracking phenomena reduce the structural integrity of buried oil and gas transmission pipelines as they are the primary deterioration mechanism under coating failure and cathodic protection. The external corrosion environment for buried pipelines often consists of moist, relatively high conductivity soils. The understanding of corrosion in underground conditions still remains unclear because soil is a porous heterogeneous environment of complex material, comprising mineral or organic solid phase, water-liquid phase, air and other gas phases. A number of factors affect the corrosion of materials in soil, namely soil type, degree of aeration, temperature, soil pH, moisture content, soil resistivity, bicarbonate, chloride and sulphate ion content, dissolved gases (e.g. carbon (IV) oxide, oxygen concentration) and the presence of microbes.

A number of researchers have developed probes to determine some physicochemical parameters of soil [5-9] viz, resistivity, redox potential, pH, soluble ion and moisture content as well as developing classifications [7-12] for the estimation of soil corrosivity. Others have carried out electrochemical studies using soils that simulated

real service conditions [13-16] or have researched on the performance of metals in solutions designed to simulate the types of physicochemical conditions that occur in soils [13,17-21]. The corrosivity of soils and in particular of soil simulating solutions has been discussed widely from both theoretical and experimental approaches [22-24]. Electrochemical methods have been used to study the corrosivity of soil environments [22]. Electrochemical parameters such as corrosion current density (I_{corr}) and polarization resistance (R_p) can be used for the evaluation of soil corrosivity given that following Ohm's law, corrosion currents are inversely proportional to soil resistivity, which is a major factor in determining soil corrosivity [24]. Furthermore, R_{ct}^{-1} (the reciprocal of the charge-transfer resistance, R_{ct}) has been extensively used in literature [17,25-27] as an index of instantaneous corrosion rate.

The objective of the study is to evaluate the corrosion of API 5L X52 pipeline carbon steel in simulated soil solutions prepared from the assessment of some soil chemical parameters in some locations in Cross River State in the Niger Delta Region of Nigeria. Thelocations chosen for the study has buried pipelines for transmitting oil, gas and water. The study examines the influence of pH and temperature on the electrochemical and corrosion behaviour of API 5L X52 carbon steel in simulated soil solutions using potentiodynamic polarization and electrochemical impedance spectroscopy (EIS). Analysis of the kinetic parameters and the mechanism that characterizes the corrosion process is discussed. The results from this work would provide supporting information on the service lifetime of pipelines, reduce failure in service and the outcomes of the assessment can be used for deciding inspection intervals and other integrity monitoring programmes.

2. Experimental details

2.1. *Pipeline Steel*

API 5L X52 carbon steel pipeline was used as the working electrode for the study. The composition of the test material is presented in Table 1. This steel is a grade of carbon steel of high strength and high toughness widely used in conveying gas, water and crude oil because of its resistance to crack propagation and it is less expensive which makes it suitable for long pipelines. The steel samples were mechanically cut into roughly (1×1×1) cm^3 cube shapes. These were wet-ground with different grit sizes (#240 - #1200) of silicon carbide emery paper using a UNIPOL- 820 metallographic lapping/polishing machine. Specimens were connected to wires by soldering and electrical conductivity was ascertained. These were mounted in epoxy resin with an exposed surface area of the specimen of 1.0 cm^2. Before each experiment, the specimens were once again ground to a smooth polished surface, followed by rinsing in distilled water, degreasing in absolute ethanol and dried.

Table 1: Elemental composition of API 5L X52 carbon steel [28]

Element	**C**	**Mn**	**Si**	**P**	**S**	**Cr**	**Ni**	**Ti**	**Nb**	**Mo**	**V**	**Al**	**Fe**
Composition wt. %	0.22	1.40	0.45	0.025	0.015	0.20	0.20	0.04	0.15	0.08	0.15	0.030	bal.

2.2. *Soil analysis and soil simulating solution*

API 5L X52 carbon Soil samples were taken from a depth of 1.1 m from the ground level from two locations in two different Local Government Areas, Akapbuyo (4°58' N, 8°30' E) and Yakurr (5°47' N, 8°4' E). They were carried in air tight polyvinyl bags to the laboratory for analysis within 24 hrs of collection from the site. Physicochemical analysis and chemical compositions of the soil from the various sites (S_1 to S_4) was established and summarized in Table 2 and 3 respectively. The chemical analysis of a specific location allows for the determination of the aggressiveness of the site and is necessary for the explanation of the corrosion mechanism model for the specific site.

Table 2: Physicochemical analysis of the soil specimens

Location	**Sand %**	**Silt %**	**Clay %**	**Moisture %**	**pH**	**EC dSm^{-1}**	**Temp. °C**
AKPABUYO LGA							
S_1	69.7	8.3	24.0	6.9	4.7	0.86	28.8
S_2	68.3	6.7	25.0	6.4	4.7	0.92	29.0
YAKURR LGA							
S_3	70.0	7.0	23.0	17.2	5.0	0.64	29.0
S_4	68.0	7.0	25.0	15.6	5.1	0.69	29.3

Table 3: Ionic composition of the soil specimens (mg/L)

Location	Ca^{2+}	Mg^{2+}	K^{+}	Cl^{-}	SO_4^{2-}	HCO_3^{-}
S_1	3.2	1.4	0.12	342	279	241
S_2	3.4	1.2	0.13	331	282	247
S_3	4.0	1.6	0.13	318	287	224
S_4	3.6	1.8	0.15	320	284	236

Test solutions were prepared by reconstitution of the chemical composition of soil in what is known as a simulated solution of soil. The choice of salts demands an inclusion of concentrations of sodium, potassium and calcium ions so that an ionic balance can be attained. S_1 and S_4 compositions have been selected for the preparation of the simulated solutions (Table 4) as they present more corrosive characters (in each locality) in terms of their average concentrations in bicarbonate, sulphate and chloride ions.

Table 4: Chemical composition of soil simulating solution (mg/L)

Location	$CaSO_4$	$MgSO_4$	K_2SO_4	NaCl	Na_2SO_4	$NaHCO_3$
S_1	3.2	1.4	0.12	342	279	241
S_4	3.6	1.8	0.15	320	284	236

2.3. *Electrochemical measurements*

Potentiodynamic polarization and Electrochemical Impedance Spectroscopy (EIS) were carried out on the samples by means of a potentiostat (Gamry Reference 600 Potentiostat/Galvanostat) and controlled by Gamry Framework and Gamry Echem Analyst softwares to obtain and analyze the measurements respectively. A conventional three-electrode cell with a saturated calomel electrode (SCE) as reference electrode and platinum as the counter electrode was used. The working electrode was the steel specimen with an exposed surface area of 1.0 cm^2. The electrode potential varied from 250 mV below E_{corr} to 700 mV above E_{corr} with a scan rate of 0.5 mV/s, for the potentiodynamic current-potential curves. These measurements were carried out over a temperature range of 30 ^oC to 50 ^oC and at pH 4.9, 7.0 and 9.0. The pH of the prepared solutions was in the range 9.4-9.7 and was adjusted by buffering with a few drops of 0.01 M HCl solution.

EIS spectra were obtained at open-circuit potential (OCP) over the frequency range of 10^5 to 0.5 Hz, at a rate of 10 points per decade using an AC signal amplitude of 10 mV. All EIS measurements were made at room temperature of 30 ^oC. Measurements were carried out three times to ensure repeatability and the results averaged for accuracy.

Results and Discussion

3.1. *Soil parameters*

Some soil parameter values derived from soil investigations are given in Table 2. The values are closely related in all locations in terms of soil nature, pH and temperature except for soil moisture and soil electrical conductivity (EC). The soil nature in all locations can be characterized as sandy clay and acidic. The soil moisture in S_3 and S_4 are higher by over two orders of magnitude than the values in S_1 and S_2. EC investigated at locations S_1 and S_2 are relatively higher than at S_3 and S_4. EC is the inverse of resistivity. Soil resistivity is an important parameter in determining soil corrosivity for buried metallic structures. Investigations by Benmoussa *et al*. [13] show decreasing soil resistivity values linked with increasing moisture content and temperature that helps in ionic exchange between the surface of the buried steel and the corrosive soil environment. While some authors have reported increasing soil aggressiveness in low resistivity soils, others [29] have recorded high corrosion rates and severe deterioration of pipeline steel in highly resistive soils. EC is dependent on the soil electrolyte composition. In the constitution of the soil simulating solution, this parameter should distinct the solutions although this measurement was not carried out. For a reliable assessment of the soil corrosivity, electrochemical investigations are required and should distinctly reveal subtle differences between the solutions.

3.2. *Potentiodynamic polarization tests*

An understanding of the corrosion kinetics was obtained from potentiodynamic polarization experiments conducted on the steel specimen in soil simulating solutions at various pH and temperature conditions.

3.2.1.*Influence of pH*

The corrosion processes taking place on the surface of buried pipelines are subject to acidic, neutral and basic soil electrolyte environments. Potentiodynamic polarization plots obtained at 30 ^oC for the steel specimen in

$S_1$and S_4 solutions in the pH range 4.9-9.0 are presented in Fig. 1. Values of the polarization parameters of corrosion potential (E_{corr}), corrosion current density (I_{corr}), polarization resistance (R_p), cathodic and anodic Tafel slopes (β_c and β_c) and corrosion rate (R_{corr}) are given in Table 5.

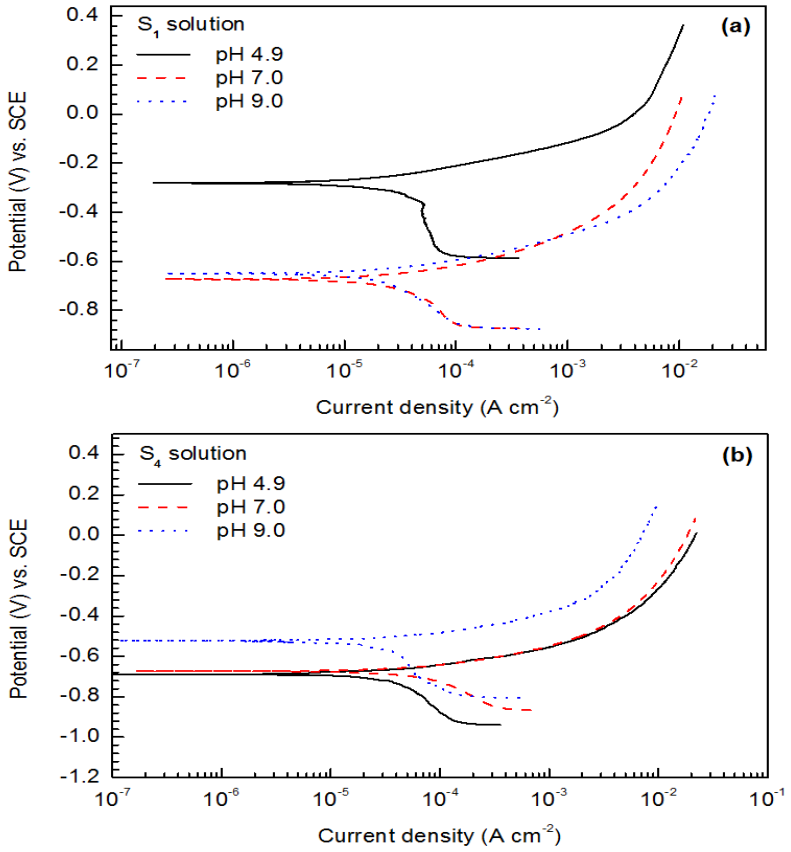

Figure 1: Potentiodynamic polarization curves of API 5L X52 carbon steel at different pH values and at 30 ^oC in (a) S_1 and (b) S_4 soil simulating solutions

Table 5: Polarization parameters of API 5L X52 carbon steel in S_1 and S_4 soil simulating solutions at 30 ^oC for pH variation in the range 4.9 – 9.0

Location	pH	E_{corr} (mV/SCE)	I_{corr} (μA/cm^2)	R_p (Ω cm^2)	β_c (mV/dec)	β_a (mV/dec)	R_{corr} (mpy)
	4.9	-280.8	49.31	956	564.1	134.3	22.53
S_1	7.0	-673.0	39.45	986	447.5	111.8	18.03
	9.0	-649.8	26.34	1264	358.6	88.96	12.03
	4.9	-688.0	64.59	509	440.4	91.5	29.51
S_1	7.0	-673.0	60.85	598	352.2	109.9	27.80
	9.0	-522.2	31.66	924	474.9	78.5	14.47

The results obtained from the polarization curves show corrosion of steel as a function of pH as increasing corrosion rates were recorded with increasing acidic conditions. Increasing R_p and decreasing I_{corr} values were observed with increasing pH values. This implies a decrease in corrosion activity as I_{corr}varies inversely with R_p. Although this trend has been noticed by researchers, it is noteworthy to mention that for small pH variations particularly at neutral or near-neutral pH, the trend is difficult to accurately recognize and large variations in pH of ±1.5 or more is required [30].

3.2.2. *Effect of temperature*

The effect to temperature on steel resistance corrosion was investigated by means of potentiodynamic polarization measurements. Fig. 2 shows the polarization curves in the temperature range 30 ^oC to 50 ^oC at pH 4.9. Values for E_{corr}, I_{corr}, R_p, β_c, β_a and R_{corr} are given in Table 6. The choice of pH of 4.9 was selected since it reflected the most extreme corrosion condition. The anodic polarization curves are seen to shift towards higher

corrosion current density values with increasing temperature. The shift however, is not so prominent in S_4 simulating solution as temperature increases from 30 ^oC to 40 ^oC. Thus, corrosion rate increases with corrosion current density. A rise in temperature of about 20 ^oC, increases the corrosion rate to about three orders of magnitude for both soil simulating solutions. In comparing the corrosion rates between S_1 and S_4 solutions, higher values are obtained for S_4 solutions. Acidic soils in particular show exponential increase in corrosion speeds with temperature due to the heightened hydrogen release from hydrogen ion reduction.

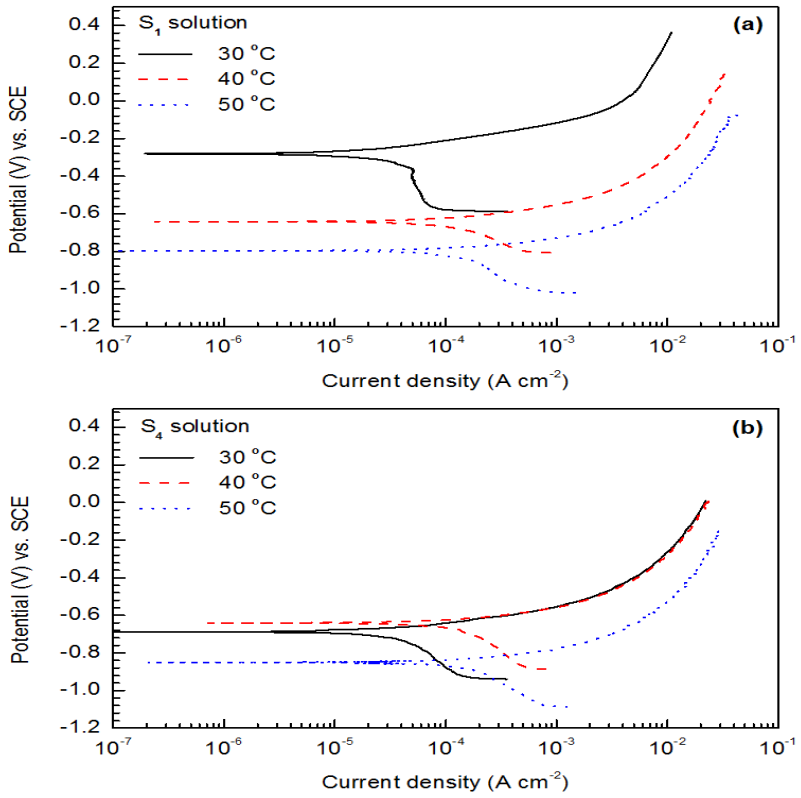

Figure 2: Potentiodynamic polarization curves of API 5L X52 carbon steel at different temperatures and at pH = 4.9 in (a) S_1 and (b) S_4 soil simulating solutions

Table 6: Polarization parameters of API 5L X52 carbon steel in S_1 and S_4 soil simulating solutions at pH = 4.9 for temperature variation in the range 30 ^oC -50 ^oC

Location	Temp (^oC)	E_{corr} (mV/SCE)	I_{corr} (μA/cm^2)	R_p (Ω cm^2)	β_c (mV/dec)	β_a (mV/dec)	R_{corr} (mpy)
S_1	30	-280.8	49.31	956	564.1	134.3	22.53
	40	-641.5	139.90	230	293.0	99.1	63.95
	50	-796.9	155.10	196	396.5	84.0	70.86
S_4	30	-688.0	64.59	509	440.4	91.5	29.51
	40	-641.0	153.00	204	480.4	84.5	69.84
	50	-850.1	184.40	194	392.9	104.1	84.24

The interactions at the electrode-electrolyte interface is modified under temperature changes resulting in changes in corrosion rates. Buried pipelines experience temperature effects under different climates and even at varying seasons leading to changes in the way the steel pipeline interacts with the conditions in the soil.
The corrosion activation energy E_a was determined from the slope of the Arrhenius plot (Fig. 3) of the natural logarithm of corrosion current density (ln I_{corr}), against the inverse of temperature (1/T) using the expression:

$$ln\, I_{corr} = -{}^{E_a}/_{RT} + lnA \qquad (1)$$

where A is the pre-exponential factor, R is the universal gas constant and T the absolute temperature. The E_a values were calculated to be 47.01 kJ mol^{-1} and 42.96 kJ mol^{-1} for S_1 and S_4 solutions respectively. These values fall within the limit of the value of the activation energy of steel corrosion in acidic soils which can reach a value of 60 kJ mol^{-1} [31, 32].

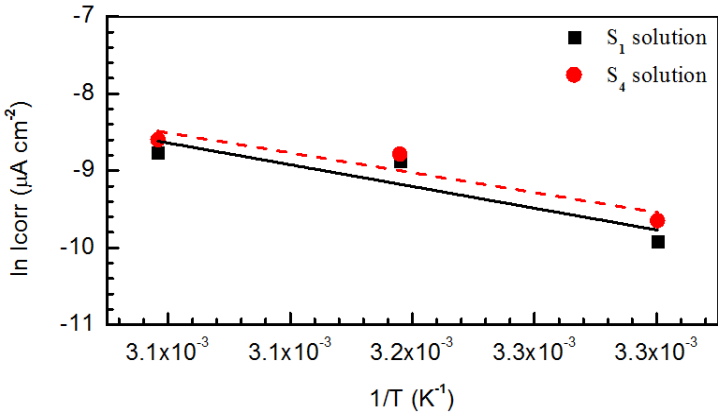

Figure 3: Arrhenius plot obtained from corrosion current density relationship with temperature for S1 and S4 soil simulating solutions (pH = 4.9)

3.3. *Electrochemical Impedance Spectroscopy*

EIS results for API 5L X52 carbon steel in S_1 and S_4 solutions at 30 ^oC and pH 4.9 for immersion times up to 24 hrs are shown in Fig. 4a-4f. These plots provide an understanding of corrosion by elucidating the electrochemical behaviour of the soil corrosion system. EIS is capable of differentiating various electrochemical processes in corrosion such as charge-transfer and mass transfer controlled processes, interfacial layers or resistance of the soil electrolyte.

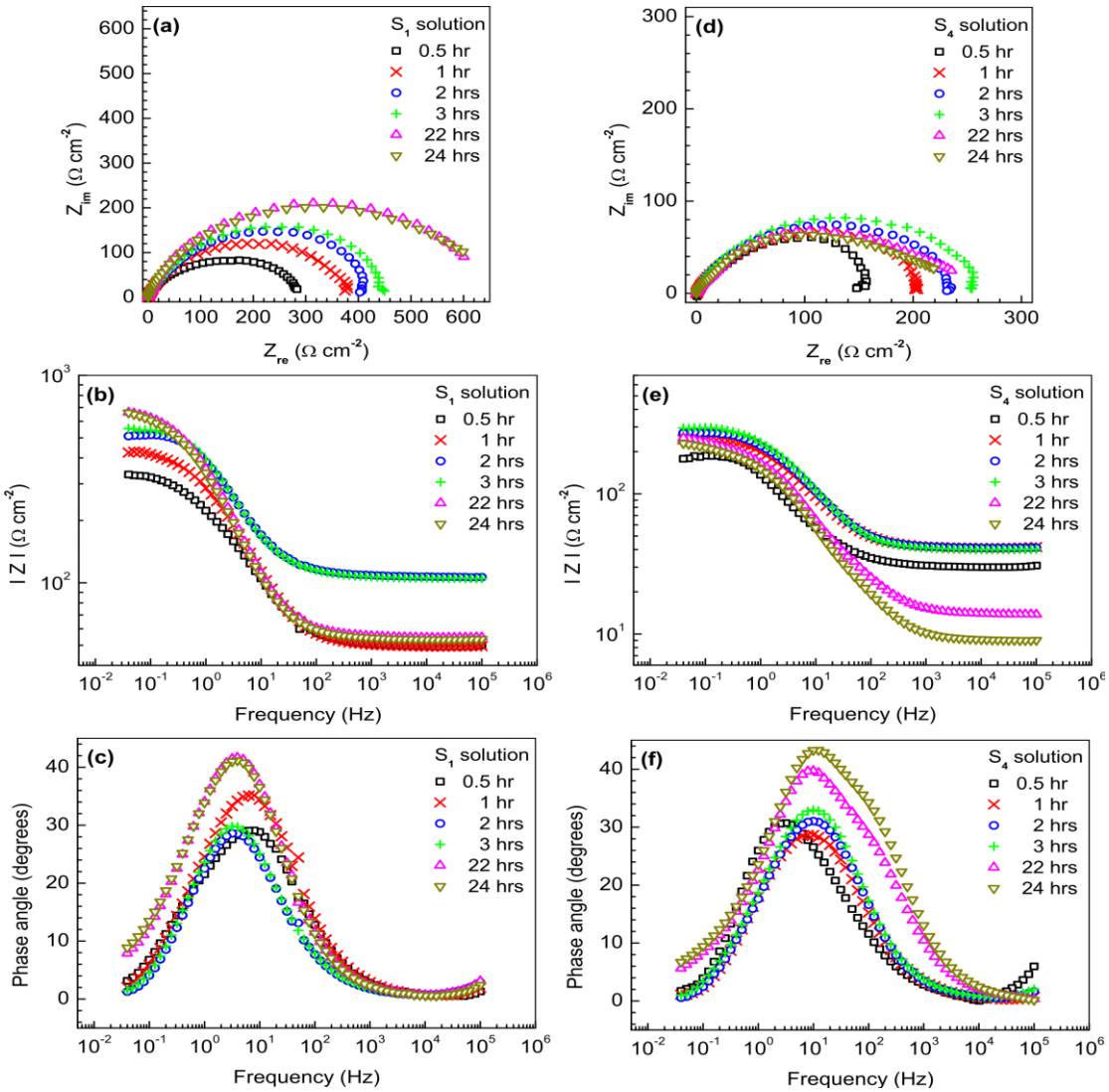

Figure 4: EIS spectra showing (a) Nyquist plots, (b) Impedance magnitude vs. frequency and (c) Bode plots for different immersion times in S_1 and S_4 soil simulating solutions at 30 ^oC and pH 4.9

The Nyquist plots of Fig. 4a and 4b show nearly-complete depressed semicircles which increase in size with increasing immersion times up to 24 hrs for S_1. In S_4 solution, the size of the loop increases steadily up to 3 hrs and shows a decrease in measurements taken after 22 hrs immersion. This suggests the presence of a protective film usually of corrosion products on the steel surface, which after sometime becomes weak. Gradually the film loses its ability to effectively protect the steel surface and the polarization resistance starts to decrease.

The impedance profile obtained in both solutions showed generally positive inflections at lower frequencies. The peaks in the Bode plot are described as distinct and the phase angle peaks shifted towards higher values at longer immersion times for both solutions. Such is characteristic of adsorption processes occurring outside the double layer as has been reported in the adsorption of bicarbonate on X100 pipeline steel [30]. Adsorption effects may also be due to relaxation of carbon carrying intermediate species [33]. The equivalent circuit model of Fig. 5 considers the adsorption resistance R_a and an adsorption constant phase element, (CPE) Q_a in addition to a charge-transfer resistance R_{ct}, a constant phase double layer Q_{dl} and the solution resistance R_s. The Constant Phase Element applied at the double layer is on account of non-ideal behaviour of the double layer capacitor, linking it to surface heterogeneities, leaky capacitor, non-uniform current distribution, etc. [34]. Hence, it replaces the double layer capacitance C_{dl} at the metal-electrolyte interface. The impedance of CPE (Z_{CPE}) is expressed as [34];

$$Z_{CPE} = [Y_0(j\omega)^n]^{-1} \qquad (2)$$

where Y_o is the CPE constant which can be converted into a capacitance, n the CPE-power ($0 < n \leq 1$), j the imaginary unit ($j = \sqrt{-1}$) and ω the angular frequency. A good fit was obtained by fitting the equivalent circuit to the experimental data as shown in Table 7 as proven by the correlation parameter χ^2.

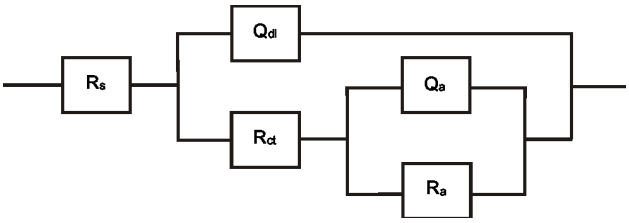

Figure 5: Equivalent electrical circuit that models the electrochemical process at the steel surface

Table 7: EIS component values for steel specimens in S_1 and S_4 solutions after different immersion times at 30 ^oC and pH = 4.9

Location	Time (hr)	R_s (Ω cm^2)	R_a (Ω cm^2)	Q_a		R_{ct} (Ω cm^2)	Q_{dl}		χ^2
				Y_0 (S s^n cm^{-2})	n_a		Y_0 (S s^n cm^{-2})	n_{dl}	
S_1	0.5	49.30	74.79	3.376×10^{-3}	0.9011	217.20	6.061×10^{-4}	0.7342	1.19×10^{-4}
	1	49.24	71.29	2.364×10^{-3}	0.9433	313.40	4.769×10^{-4}	0.7622	1.81×10^{-4}
	2	107.30	244.70	2.765×10^{-4}	0.8552	180.00	3.312×10^{-4}	0.7945	2.67×10^{-4}
	3	105.40	354.50	2.061×10^{-4}	0.7934	106.00	3.129×10^{-4}	0.7886	2.21×10^{-4}
	22	54.57	217.90	4.744×10^{-3}	0.3803	510.00	5.019×10^{-4}	0.7774	1.54×10^{-4}
	24	53.45	223.50	4.725×10^{-3}	0.4962	491.10	5.201×10^{-4}	0.7774	8.29×10^{-5}
S_4	0.5	30.28	108.60	8.180×10^{-4}	0.9247	52.95	6.793×10^{-4}	0.8012	8.38×10^{-4}
	1	41.08	74.54	9.448×10^{-4}	0.9273	133.70	4.642×10^{-4}	0.7676	9.26×10^{-5}
	2	41.04	61.90	1.291×10^{-3}	0.9260	175.00	4.305×10^{-4}	0.7693	1.26×10^{-4}
	3	39.92	51.11	1.971×10^{-3}	0.9278	210.30	4.416×10^{-4}	0.7623	1.16×10^{-4}
	22	13.57	12.18	2.341×10^{-1}	1.000	240.10	1.002×10^{-3}	0.6541	4.56×10^{-4}
	24	8.82	21.95	1.318×10^{-1}	1.000	218.30	1.007×10^{-3}	0.6750	4.52×10^{-4}

The kinetics of the electrochemical process can be described as a combination of both adsorption and charge-transfer controlled processes. S_1 and S_4 soil simulating solutions are a complex mix of chloride, sulphate and bicarbonate ions. The addition of chloride and sulphate ions to NS4 simulated soil solution has been reported to inhibit free corrosion, i.e. a reduction in open circuit potential on addition of these ions [30] and EIS spectra showed that these ions induced adsorption to the electrochemical process occurring at the metal-solution

interface. A decreasing R_a suggests an increased adsorption. Q_a increases under such conditions indicating a capacitive adsorption region in close proximity to the specimen surface which behaves similar to the double layer. This adsorption region becomes prevalent at conditions favouring adsorption. The inverse relationship between R_a and Q_a is most obvious in S_4 solution (Table 7). Figure 6 shows the corrosion activity of the steel specimen with time in both solutions. As R_a decreases, the charge transfer resistance R_{ct} increases and vice versa. The trend is apparent in S_4 solution (Figure 6b). A decreasing R_a favours more adsorption, hindering electrochemical reactions at both anodic and cathodic sites and increasing R_{ct}. Likewise, an increase in R_a leads to reduced adsorption, less coverage of adsorbed species on the metal surface, thus exposing cathodic and anodic area and facilitating charge transfer processes, implying a reduction in R_{ct}. The low frequency impedance known as the Nernst impedance [27] is often used to describe the corrosion of steel. This value is reflected here as the sum of R_a and R_{ct} and shown in Fig. 6. Higher impedance is observed for S_1 solution, making it a less corrosive solution. This corroborates the results obtained from potentiodynamic polarization measurements.

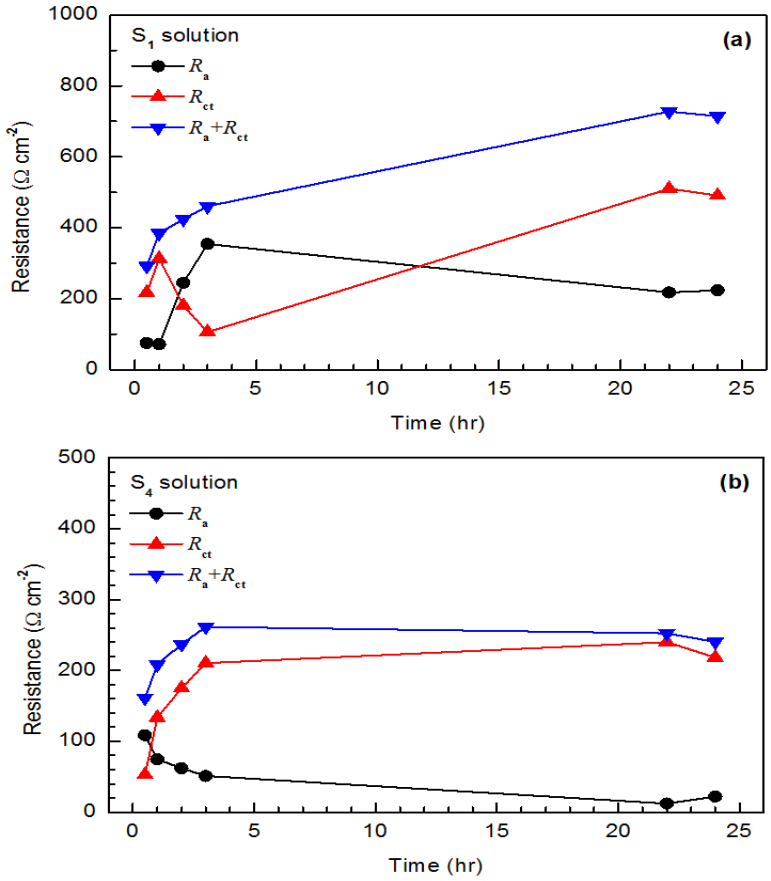

Figure 6: Corrosion activity versus immersion time based on resistance values obtained from fitting experimental data to equivalent circuit

Conclusions

Electrochemical corrosion tests were performed on API 5L X52 pipeline steel in soil simulating solutions at different pH, temperature and immersion times. The results show the reliability of electrochemical corrosion testing methods in assessing the corrosion tendencies in soil simulating solutions even for seemingly, closely related ionic concentrations of these solutions. Potentiodynamic polarization results showed an increase in steel corrosion associated with a decrease in polarization resistance as pH decreased. In the temperature range studied, corrosion current density increases with increasing temperature for both soil simulating solutions, and the steel corrosion potential moves towards negative values as temperature increases from 30 ^{o}C to 50 ^{o}C. EIS data generally revealed larger polarization resistance values with immersion time for S_1, whereas for S_4, relatively smaller polarization resistance values were observed indicating lower corrosive nature of S_1 solution. An equivalent circuit model consisting of a double layer and an adsorption constant phase element characterized the kinetics of the electrochemical process occurring at the interface between the steel surface and the solution as jointly adsorption and charge-transfer controlled. The results of corrosion rates obtained from

potentiodynamic polarization measurements and polarization resistance values form EIS clearly reveals S_4 solution as being more corrosive than S_1 solution. Thus, soil corrosivity can be ascertained from analysis carried out on soil simulating solutions. Using this approach, the structural integrity of pipeline steel structures can be evaluated form corrosion resistance studies performed on soil simulating solutions.

Acknowledgments - M. E. Ikpi acknowledges China-Africa Science and Technology Partnership Program (CASTEP), for the 2012 Award for Equipment donation. This research carried out at the CER-Laboratory, Department of Pure and Applied Chemistry, University of Calabar, Nigeria was made possible through that support from CASTEP.

References

1. Olokesusi F., Environmental Impact Analysis and the Challenge of Sustainable development in the Oil Producing Communities, NITP Abuja, (2005).
2. Handasah D., Bonny Master Plan - Final Draft Existing Report, NITP Port-Harcourt, (2003).
3. Adejoh O.F., *World Environ.* 4 (2014) 93.
4. Niger Delta Development Commission (NDDC), Sustainable Livelihoods and Job Creation, NDDC Port-Harcourt, (2001).
5. Li M. C., Han Z., Lin H. C., Cao C.N., *Corr.* 57 (2001) 913.
6. Constanzo F. E., MecvVey R.E., *Corrosion – NACE* 14 (1958) 269T.
7. Booth G. H., Cooper A. W., Cooper P. M., Wakerley D.S., *Brit. Corros. J.* 2 (1967) 104.
8. Booth G. H., Cooper A. W., Cooper P.M., *Brit. Corros. J.* 2 (1967) 109.
9. Booth G.H., Cooper A. W., Tiller A.K., *Brit. Corros. J.* 2 (1967) 114.
10. Stumm W., Morgan J.J., Aquatic Chemistry, Second Edition, Wiley Interscience, 1981.
11. Uhlig H. H., Revie R.W., Corrosion and Corrosion Control - An Introduction to Corrosion Science and Engineering, John Wiley & Sons, 1985.
12. Macdonald D.D., Transients Techniques in Electrochemistry, Plenum, 1977.
13. Benmoussa A., Hadjel M., Traisnel M., *Mater. Corros.* 57 (2006) 771.
14. Belmokre K., Azzouz N., Kermiche F., Wery M., Pagetti J., *Mater. Corros.* 49 (1998) 108.
15. Kasahara K., Kajiyama F., *Corros.* 39 (1983) 475.
16. Nie X. H., Li X.G., Du C. W., Cheng Y.F., *J. Appl. Electrochem.* 39 (2009) 277.
17. Yan M., Sun C., Xu J., Ke W., *Ind. Eng. Chem. Res.* 53 (2014) 17615.
18. Scully J. R., Bundy K.J., *Mater. Perform.* 24 (1985) 18.
19. Wu Y. H., Liu T. M., Luo S. X., Sun C., *Materialwiss. Werkstofftech.* 41 (2010) 142.
20. Wu Y. H., Liu T. M., Sun C., Xu J., Yu C.K., *Corros. Eng. Sci. Technol.* 45 (2010) 136.
21. Liu T. M., Wu Y. H., Luo S. X., Sun C., *Materialwiss. Werkstofftech.* 41 (2010) 228.
22. Antunes de Suna R., Bastos I. N., Platt G.M., *ISRN Chem. Eng.* (2012), doi: 10.5402/2012/103715.
23. Velazquez J. C., Caleyo F., Valor A., Hallen J.M., *Corros.* 65 (2009) 332.
24. Ferreira C.A. M., Ponciano J.A. C., Vaitsman D. S., Perez D.V., *Sci. Total Environ.* 388 (2007) 250.
25. Yan M., Sun C., Xu J., Dong J., Ke W., *Corros. Sci.* 80 (2014) 309.
26. Wu T., Xu J., Sun C., Yan M., Yu C., Ke W., *Corros. Sci.* 88 (2014) 291.
27. Thee C., Hao L., Dong J. H., Mu X., Wei X., Li X., Ke W., *Corros. Sci.* 78 (2014) 130.
28. ASTMSpec, SPEC 5L Specification for line pipe, 14th edition, West Conshohocken, 2013.
29. Cao C.N., Material Corrosion in Natural Environment of China, Chemical Industry Press, 2005.
30. Gadala I. M., Alfantazi A., *Corros. Sci.* 82 (2014) 45.
31. Larabi L., Harek Y., Benali O., Ghalem S., *Progr. Org. Coat.* 54 (2005) 256.
32. Selles C., Benali O., Tabti B., Larabi L., Harek Y., *Mater. J. Environ. Sci.* 3 (2012) 206.
33. Wu S. L., Cui Z. D., Zhao G. X., Yan M. L., Zhu S. L., Yang X.J., *Appl. Surf. Sci.* 228 (2004) 17.
34. El-Sayed M., Sherif M., Almajid A., Khalil A., Junaedi H., Latief H., *Int. J. Electrochem. Sci.* 8 (2013) 9360